



Discovery of a novel family of FKBP12 “reshapers” and their use as calcium modulators in skeletal muscle under nitro-oxidative stress



Jesus M. Aizpurua^{a,*}, José I. Miranda^a, Aitziber Irastorza^a, Endika Torres^a, Maite Eceiza^a, Maialen Sagartzazu-Aizpurua^a, Pablo Ferrón^b, Garazi Aldanondo^{c,d}, Haizpea Lasa-Fernández^{c,d,e}, Pablo Marco-Moreno^{c,d}, Naroa Dadie^e, Adolfo López de Munain^{c,d,e}, Ainara Vallejo-Illarramendi^{c,d,e,**}

^a Joxe Mari Korta R&D Center, Departamento de Química Orgánica-I, Universidad Del País Vasco UPV/EHU, Avda. Tolosa-72, 20018, San Sebastián, Spain

^b Miramoon Pharma S.L., Avda Tolosa-72, 20018, San Sebastián, Spain

^c Instituto de Investigación Sanitaria Biodonostia, Grupo de Enfermedades Neuromusculares, Paseo Dr Begiristain s/n, 20014, San Sebastián, Spain

^d CIBERNED, Instituto de Salud Carlos III, 28031, Madrid, Spain

^e Grupo de Neurociencias, Departamentos de Pediatría y Neurociencias, Universidad Del País Vasco UPV/EHU, Hospital Donostia, Paseo Dr Begiristain S/n, 20014, San Sebastián, Spain

ARTICLE INFO

Article history:

Received 6 October 2020

Received in revised form

23 December 2020

Accepted 4 January 2021

Available online 14 January 2021

Keywords:

Ryanodine receptor

Triazoles

Calcium channel

ABSTRACT

The hypothesis of rescuing FKBP12/RyR1 interaction and intracellular calcium homeostasis through molecular “reshaping” of FKBP12 was investigated. To this end, novel 4-arylthioalkyl-1-carboxyalkyl-1,2,3-triazoles were designed and synthesized, and their efficacy was tested in human myotubes. A library of 17 compounds (**10a-n**) designed to dock the FKBP12/RyR1 hot-spot interface contact residues, was readily prepared from free α -amino acids and arylthioalkynes using CuAAC “click” protocols amenable to one-pot transformations in high overall yields and total configurational integrity. To model nitro-oxidative stress, human myotubes were treated with the peroxynitrite donor SIN1, and evidence was found that some triazoles **10** were able to normalize calcium levels, as well as FKBP12/RyR1 interaction. For example, compound **10b** at 150 nM rescued 46% of FKBP12/RyR1 interaction and up to 70% of resting cytosolic calcium levels in human myotubes under nitro-oxidative stress. All compounds **10** analyzed showed target engagement to FKBP12 and low levels of cytotoxicity *in vitro*. Compounds **10b**, **10c**, **10h**, and **10iR** were identified as potential therapeutic candidates to protect myotubes in muscle disorders with underlying nitro-oxidative stress, FKBP12/RyR1 dysfunction and calcium dysregulation.

© 2021 Elsevier Masson SAS. All rights reserved.

1. Introduction¹

Intrinsically slow secondary amide rotations in proline peptides can be catalyzed by rotamerase enzymes to elicit a reversible protein backbone switch from the open (*trans*-) to the closed (*cis*-) state to activate transmembrane ion channels [1]. In particular FKBP12, also known as Calstabin1, is a peptidyl-prolyl isomerase (PPIase) expressed in the cytosolic region of skeletal muscle, among other tissues, and is thought to catalyze the *trans/cis* inter-

conversion of a still not precisely identified Xxx–Pro segment in the FKBP-binding domain of ryanodine receptor RyR1 [2]. This channel regulates the periodical efflux of calcium ions from the sarcoplasmic reticulum (SR) to the actin-myosin contraction system and is critical in excitation-contraction coupling (EC). RyR1 malfunction, generally caused by congenital mutations, may lead to “leaky” calcium channels that are related to severe muscle conditions [3–5]. In addition, the FKBP12/RyR1 interaction can also be altered or compromised by post-translational chemical modifications of RyR1 residues placed close to the switching Xxx–Pro segment. For example, S-nitrosylation of RyR1 cysteine residues caused by the aberrant activity of nitric oxide synthase (nNOS) enzyme [6], exhausting exercise, or aging, is known to interfere with the proper closing of ryanodine receptor channels, and results in calcium ion leakage in skeletal muscles [7].

* Corresponding author.

** Corresponding author. Grupo de Neurociencias. Departamento de Pediatría, UPV/EHU, Paseo Dr Begiristain s/n, 20014, San Sebastián, Spain.

E-mail addresses: jesusmaria.aizpurua@ehu.eus (J.M. Aizpurua), ainara.vallejo@ehu.eus (A. Vallejo-Illarramendi).

Two structures of mammalian RyR1 channels bound to FKBP12 in both open and closed conformations have been recently elucidated at a near-atomic resolution [8,9]. These structures have provided an unprecedentedly detailed explanation for the long-range allosteric regulation of calcium ion conductance of tetrameric RyR1 channels following a complex cascade of synchronized conformational changes [10,11]. Despite these remarkable advances, the molecular clues behind the rotamerase activity of FKBP12 on RyR1 remain obscure. The generally accepted mechanism for the rotamerase action of FKBP12 involves the stabilization of a twisted prolyl amide transition state with a key $C\alpha_{Xxx}-CO_{Pro}-N_{Pro}-C\alpha_{Pro}$ dihedral angle of about 90° in the isomerizable protein [12]. FKBP12 is estimated to accelerate the *trans/cis* transformation by 10^4 fold compared to the uncatalyzed isomerization [13,14].

Rapamycin and immunosuppressant FK506 are the most efficient known inhibitors of FKBP12 and both contain in their structures a central L-pipecolic acid residue strained to 98° and 95° respectively by rigid macrocyclic structures. This motif has inspired the synthesis of many low molecular weight FKBP12 ligands aimed to elicit effective immunosuppression [15]. However, rapamycin, FK506 and most of the L-pipecolic acid peptide surrogates displace FKBP12 from RyR1 channels, resulting in an increased calcium leakage through RyR1 from the SR into the cytosol [16]. On the other hand, different studies have demonstrated the beneficial effects of RyR1 channel stabilizers on animal models of muscular dystrophy. For instance, benzothiazepines JTV519/K201 [17], S107 [18] and S48168/ARM210 [19], also known as “rycals”, have reportedly improved *in vivo* muscle function and exercise performance in the *mdx* Duchenne muscular dystrophy mouse model. Such compounds decrease the Ca^{2+} leakage from the SR by preventing FKBP12 depletion from RyR1 channels. However, the mechanistic details of their activity are poorly understood [20].

In order to seek additional evidence on the nature of the key amino acids involved in the molecular mechanism of the FKBP12/RyR1 interaction and the deleterious effect caused by the S-nitrosylation of putative cysteine residues, we decided to conduct a combined computational and experimental study. Our objective was to modify such protein-protein interaction using selective ligands of FKBP12 that cause a “reshaping” of its surface and, therefore, a potential restoration of the peptidyl-prolyl isomerase activity of FKBP12 when RyR1 is hyper-nitrosylated. Herein we report the design and synthesis of a novel family of 1,2,3-triazole-based reshapers of FKBP12 and their biological activity as stabilizers of FKBP12/RyR1 interaction and modulators of cytosolic calcium concentration in human myotubes submitted to chemical nitro-oxidative stress.

2. Results and discussion

2.1. Design

The crystal structure of the FKBP12/RyR1 tetramer complex (Protein Data Bank code 3J8H) [9] was used as the starting point to design triazole ligands suitable to modify the protein-protein interaction (PPI). A successful modulator ligand should dock the critical interaction surface areas by binding together several amino acid hot-spots. The identification of such key residues was conducted computationally using the virtual alanine scanning approach, which provides interaction energy differences for individual residues upon simulated mutation to alanine.

After subjecting the FKBP12/RyR1 complex to virtual alanine scanning by using the DrugScore PPI server [21] and setting the cut-off value at $\Delta\Delta G > 1.5$ kcal mol $^{-1}$, we identified two groups of FKBP12 residues involved in the protein-protein interaction. One

group was formed by the polar Asp-37 and Arg-42 residues participating in a pocket of electrostatic interactions, and the second one comprised the Tyr-82 and Ile-90 residues engaged in hydrophobic interactions. The counterpart RyR1 interface amino acids include the Asp-1690 residue and the segment Pro-1780, Cys-1781, Phe-1782, Val-1783 (Fig. 1A).

After identifying the hot-spot cluster, several triazole structures **10** were designed as potential ligands to simultaneously fit the ionic and the hydrophobic pockets of the FKBP12/RyR1 complex (Fig. 1B). Recently, 1*H*-1,2,3-triazoles have proved to be suitable scaffolds for small drug development [22]. Furthermore, such compounds would be easily accessible from the clicking of substituted thio-phenol propargyl sulfides and α -azido azides (see below, Scheme

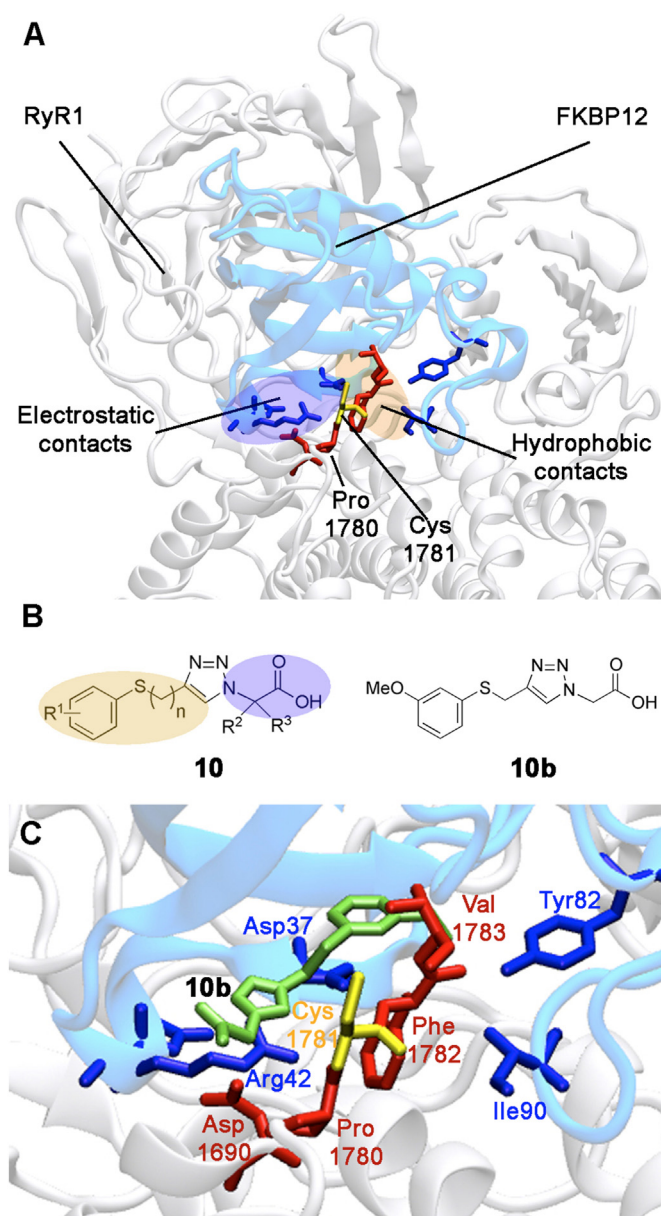
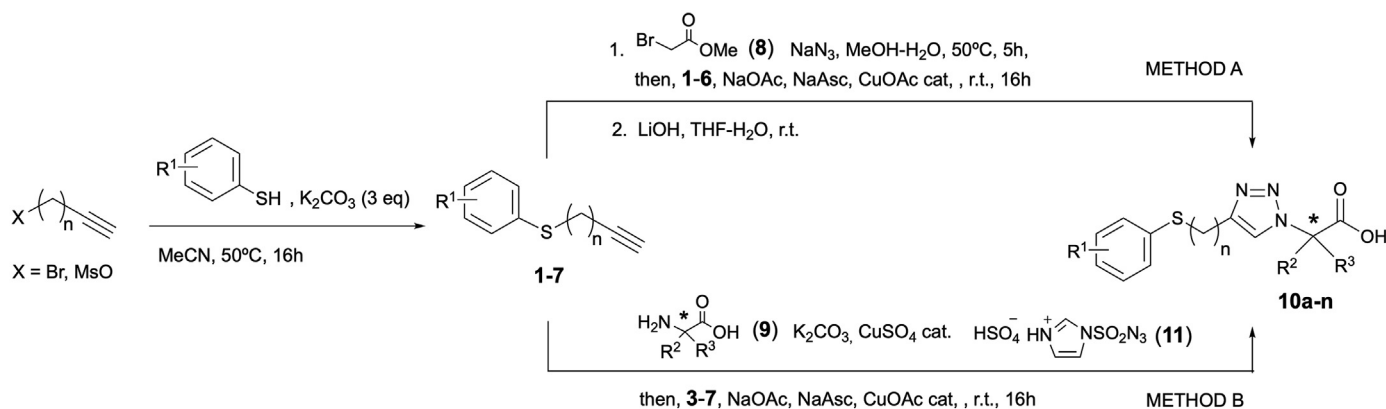


Fig. 1. (A) FKBP12/RyR1 interaction (PDB ID: 3J8H) [9]. Hot-spot residues ($\Delta\Delta G > 1.5$ kcal mol $^{-1}$) obtained after virtual alanine scanning are shown in blue for FKBP12, and in red for RyR1. Electrostatic and hydrophobic contact pockets are highlighted in purple and orange, respectively. (B) Triazoles studied in this work (general structure **10**) designed to incorporate polar (purple) and hydrophobic (orange) fragments. (C) Docking of ligand **10b** (in green) to the FKBP12/RyR1 complex. For a detailed 2D interaction diagram of **10b**, see Supplementary Material (S3).

Scheme 1. Synthesis of triazoles **10a-n**.

1). To check this hypothesis, we conducted a computational docking study using the Autodock FR [23] software package. Proteins and ligands were prepared using the AutoDock Tools 1.5.7 software following standard protocols. The selection of the docking area and mobile side-chains in the FKBP12/RyR1 was achieved using the AutoGrid FR software. This area was limited to the residues Tyr-26, Phe-36, Asp-37, Phe-46, Phe-48, Glu-54, Trp-59, Phe-99 (in FKBP12) and Phe-1782, Val-1783 (in RyR1). All these residues surround the key interaction of amino acids Arg-42 (in FKBP12) and Pro-1780 (in RyR1), which are placed in the center of a characteristic groove-like structure. The RyR1 protein docking surface was limited to the 1777–1783 residues comprising a peptide loop interacting with the FKBP12 groove. Each ligand was docked 50 times to obtain average interaction energies.

As exemplified in Fig. 1C for ligand **10b**, such triazoles repeatedly docked the FKBP12/RyR1 complex hot-spot interface with typical docking energies in the range of 12–14 kcal mol⁻¹ showing a uniform spatial disposition. In particular, compound **10b** was found to form two hydrogen bonds with the Tyr-26 and His-87 residues of FKBP12 and a weak interaction with the Cys-1781 residue of RyR1 (see Supplementary Material (S3)). Considering that this ligand contains the minimum essential groups for activity, we chose it as a representative model of compounds **10** to conduct target engagement experiments with FKBP12 complexes (see below). Furthermore, we hypothesized that triazole ligands **10** could modulate the long-range allosteric effect elicited by FKBP12 on RyR1 channels.

2.2. Chemistry

For the preparation of triazoles **10** (Scheme 1) we developed several one-pot protocols starting from alkynes **1–7** which, in turn, were easily obtained in 56–99% yields from propargyl bromide or homopropargyl alcohol mesylate by a nucleophilic substitution reaction with several thiophenols under basic conditions. Copper(I)-catalyzed CuAAC reaction of arylthioalkyl alkynes **1–7** with suitable α -azido acid derivatives [24] was performed in two complementary ways. To synthesize achiral triazoles **10a-f** (Method A), methyl bromoacetate **8** was transformed with sodium azide into methyl azidoacetate and was “clicked” *in situ* with alkynes **1–6** affording the corresponding intermediate 1-methoxycarbonylmethyl-1,2,3-triazole esters. Subsequent saponification of the CO₂Me group with lithium hydroxide provided the free carboxylic acids in good to excellent overall yields (Table 1, entries 1–6). The hindered triazole **10g** (entry 7) was prepared similarly starting from methyl α -bromoisobutyrate. Finally, chiral triazoles **10h-n** (Table 1, entries 8–17) were synthesized from free α -amino acids upon Cu(II)-catalyzed diazotization to the requisite

intermediate α -azido acids using imidazole-1-sulfonylazide hydrogenosulfate **11**, followed by CuAAC reaction with the corresponding alkynes (Method B) [25]. It is worth mentioning that triflyl azide proved to be an unsuitable N-diazotation reagent to conduct the last transformations because, after the workup, inseparable mixtures of carboxylic triazoles and triflamide were obtained. The chiral integrity of compounds **10h-n** was assessed by analytical HPLC using a chiral stationary phase (Supplementary Material S32–S42).

2.3. Pharmacology

First, we aimed to verify the target engagement of triazole ligands **10** to FKBP12. To do this, we used a well-characterized protein fragment complementation assay where the rapamycin-inducible FKBP/FRB interaction produces quantitative luminescence, due to the association of luciferase fragments fused to FKBP12 and FRB proteins. Indeed, this assay has been previously used to determine binding kinetics underlying drug action [26]. In this system, FKBP12 binds rapamycin with high affinity and then the FKBP-rapamycin complex binds FRB to form a ternary complex [27]. The addition of rapamycin to cells co-expressing FKBP12 and FRB fusion proteins resulted in an instantaneous increase of luminescence of around 2 orders of magnitude (Fig. 2B). The observed potency of rapamycin to induce protein dimerization (EC₅₀ value) was 36.39 nM (Fig. 2C), which is in agreement with previously published data [27]. As expected, neither FK506 nor triazole **10b** were able to induce FKBP12/FRB dimerization, even at high concentrations (100 μ M and 10 mM respectively), since none of them present the rapamycin site that binds to FRB (Fig. 2A, blue residues).

We next wanted to evaluate the effect of FK506 and triazoles **10** on the FKBP/rapamycin/FRB ternary complex. Since this protein fragment complementation assay is reportedly reversible and robust for more than 1 h [27], we designed a competition assay where FK506 or triazoles **10** were added after rapamycin induction of FKBP/FRB dimerization (Fig. 2D for schematics). Hence, both FK506 and triazoles **10** would compete with rapamycin for FKBP12 binding pocket. Indeed, we found that these compounds displace rapamycin from FKBP12 with a potency (IC₅₀) of 38.29 μ M and 3.32 mM, respectively (Fig. 2E). We next wanted to determine whether other triazoles **10** also bind to FKBP12. To do so, we performed a competitive binding assay with all different triazole **10** compounds. In this assay, we used a supramaximal concentration of rapamycin (1.2 μ M) and the effect of triazole compounds (3 mM) were determined subsequently (Fig. 2F). All tested compounds **10** showed target engagement to FKBP12, as shown by the decay observed in the rapamycin-induced FKBP12/FRB dimerization,

Table 1
Preparation of triazole ligands **10a-n**.

Entry	Alkyne	R ¹	R ²	R ³	n	Config.(*)	Product	Method	Yield (%) ^a
1	1	H	H	H	1	—	10a	A	80
2	2	3-MeO	H	H	1	—	10b	A	74
3	3	4-MeO	H	H	1	—	10c	A	88
4	4	3-Cl	H	H	1	—	10d	A	67
5	5	4-Me	H	H	2	—	10e	A ^b	68
6	6	2,3,5,6-F ₄	H	H	1	—	10f	A	91
7	3	3-MeO	Me	Me	1	—	10g	A ^c	72
8	3	3-MeO	H	Bn	1	(R)	10hR	B	76
9	3	3-MeO	H	Bn	1	(S)	10hS	B	73
10	3	3-MeO	H	iBu	1	(R)	10iR	B	80
11	3	3-MeO	H	iBu	1	(S)	10iS	B	75
12	3	3-MeO	H	iPr	1	(R)	10jR	B	69
13	3	3-MeO	H	iPr	1	(S)	10jS	B	65
14	7	3-F ₃ C	H	Bn	1	(R)	10kR	B	63
15	7	3-F ₃ C	H	4-HOC ₆ H ₄ CH ₂	1	(R)	10mR	B	73
16	7	3-F ₃ C	H	4-HOC ₆ H ₄ CH ₂	1	(S)	10mS	B	86
17	4	3-Cl	H	BocHN(CH ₂) ₄	1	(S)	10nS	B	63

^a Overall yields of pure isolated products.^b From homopropargyl mesylate.^c From methyl α -bromoisobutyrate (see experimental section).

which was in the range of 20–100%.

In order to prove the mechanism of action and efficacy of novel FKBP12/RyR1 interaction stabilizers, we need specific *in vitro* models that recapitulate disease phenotypes with the involvement of nitro-oxidative stress (e.g. Duchenne muscular dystrophy). In this regard, the peroxyxynitrite donor SIN1 [28] (3-morpholino-sydoniminium chloride) can be used to induce post-translational S-nitrosylation of RyR1 *in vitro* and generate cellular models of FKBP12 depletion that are useful to test drug candidates targeting these processes. Aerobic decomposition of SIN1 produces superoxide anion (O₂^{•-}) and nitric oxide (NO[•]), which react to form peroxyxynitrite anion and induce the S-nitrosylation of cysteine residues, leading to alterations in intracellular calcium homeostasis [29]. On the other hand, *in situ* Proximity Ligation Assay (PLA) is a technique that allows direct detection of protein interactions and modifications with high specificity and sensitivity. It can readily detect, localize and quantify two interacting proteins located within 30–40 nm in unmodified cells and tissues [30]. This is achieved by using species-specific secondary antibodies linked to complementary oligonucleotides that hybridize in close proximity. Upon subsequent addition of a ligase, a polymerase, and a labeled complementary oligonucleotide, distinct bright spots are obtained, which can be imaged and quantified by fluorescence microscopy. Taking this background into account, we surmised the convenience of applying the *in situ* PLA technique in human myotubes to evaluate the effect of the S-nitrosylation stress caused by SIN1 on FKBP12/RyR1 co-localization (see Experimental for details).

As shown in Fig. 3, the FKBP12/RyR1 interaction was specifically quantified by *in situ* PLA. In healthy human myotubes, SIN1 treatment induced a 60% reduction of FKBP12/RyR1 co-localization (39.87 ± 8.46%) compared to non-stressed myotubes (100 ± 9.80%; P < 0.05). This reduction was similar to the one observed in myotubes treated with rapamycin (46.63 ± 2.96%), which upon binding to FKBP12 [31] depletes FKBP12 from RyR1 complexes [15]. Pre-treatment of myotubes with the RyR1 stabilizer S107 resulted in a partial recovery of FKBP12/RyR1 interaction, as shown by an 84% increase in FKBP12/RyR1 co-localization compared to non-treated myotubes stressed with SIN1 (from 39.87 ± 8.46 to 73.30 ± 6.26%; P < 0.05). Similarly, **10b** pre-treatment resulted in a significant increase of FKBP12/RyR1 co-localization in SIN1-stressed myotubes (from 39.87 ± 8.46% to 67.45 ± 9.55%; P < 0.05). As expected, neither S107 nor **10b** altered

FKBP12/RyR1 interaction in non-stressed control myotubes (see Supplementary Material, Fig. S1).

Our results indicate that both compounds, **10b** and S107, show efficacy in the rescue of FKBP12 depletion from RyR1 complexes that occurs in human myotubes under nitro-oxidative stress. Indeed, at 150 nM, **10b** and S107 compounds showed similar recovery of FKBP12/RyR1 interaction, corresponding to 46% and 56% recovery scores, respectively. Furthermore, our data confirm that human myotubes stressed with SIN1 mimic the FKBP12 depletion from RyR channels that result in “leaky” RyR1 channels, which is reportedly caused, among other things, by RyR1 S-nitrosylation.

We then carried out further *in vitro* experiments for direct determination of the effect of these ligands on intracellular calcium levels. Human myoblasts were differentiated into myotubes and pretreated with the benzothiazepine S107 and triazole ligands **10a-n** at 150 nM. Then, myotubes were subjected to nitro-oxidative stress with 5 mM SIN1 and after 6 h, calcium levels were determined using the ratiometric fluorochrome Fura-2AM, which measures cytosolic calcium concentration in living cells (see Fig. 4A for schematics).

In agreement with previous reports [17], a submicromolar concentration of S107 partially rescued the higher cytosolic calcium ion levels observed in SIN1-stressed human myotubes. In this line, several triazole ligands **10** displayed a similar regulating effect on the S-nitrosylated FKBP12/RyR1 complex. For example, achiral compounds **10a-10g**, derived from azidoglycine and α -azidoisobutyric acid, showed recovery scores up to 90% when the aromatic ring was substituted by electron-donating R¹ groups (e. g. MeO). Electron-withdrawing groups showed much less activity (e. g. **10d**). This last trend persisted in chiral ligands **10k-n** derived from phenylalanine, tyrosine and lysine. An exception of such tendency was the tetrafluorinated compound **10f**. However, such apparent bias change could be more related to the highly hydrophobic nature of the 2,3,5,6-tetrafluorophenyl moiety than to the electron-withdrawing effect of fluoro groups. The effect of chirality was also checked by comparing the enantiomer pairs of ligands **10h-j** and **10m**. Interestingly, compared to S enantiomers, we observed higher calcium-modulating activities of R enantiomers in all instances, excepting the phenylalanine-derived triazoles **10hR** and **10hS**, which showed similar activity.

Finally, we evaluated the *in vitro* cytotoxicity profile of selected triazoles **10** in human myoblasts by using the lactate

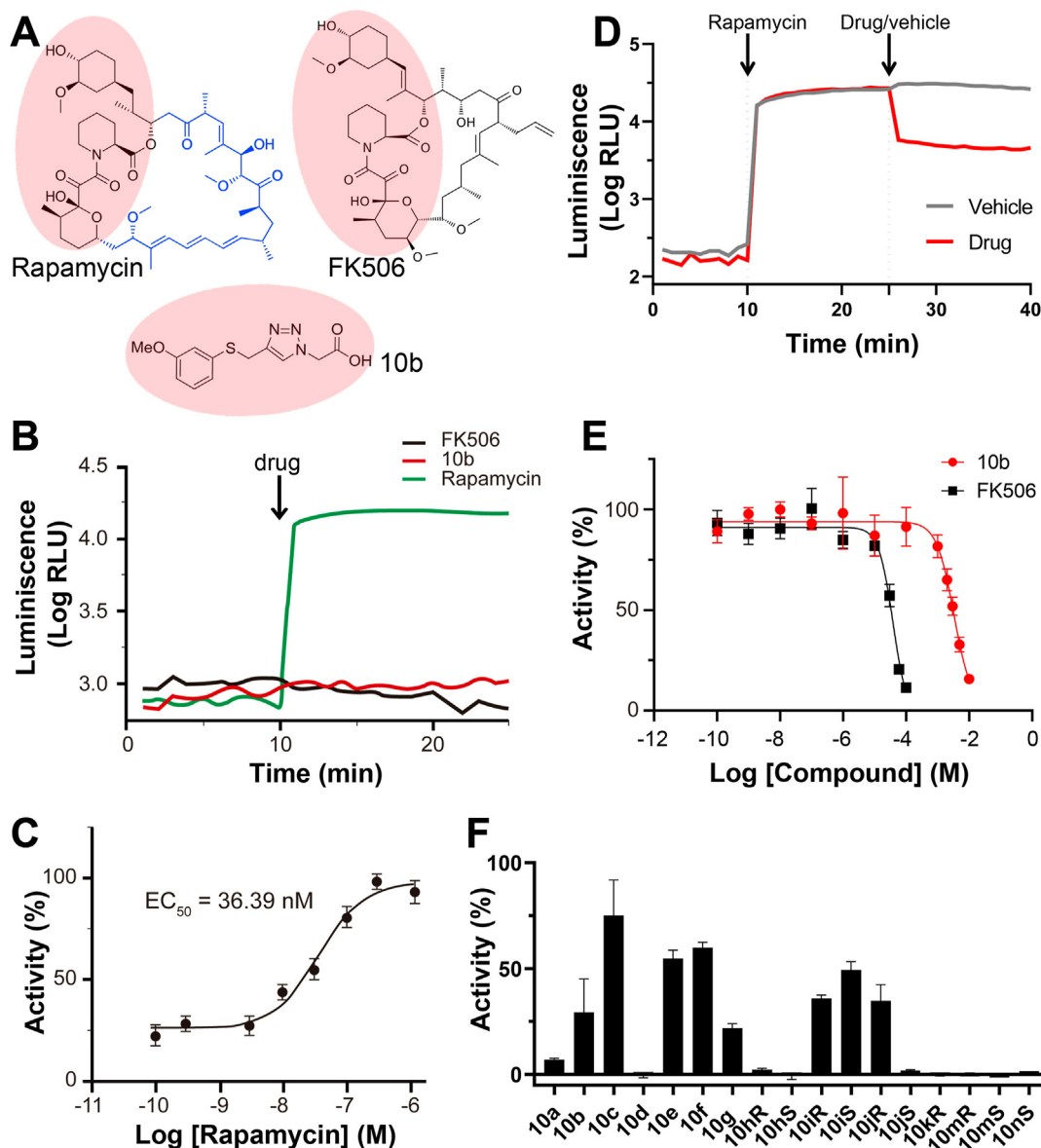


Fig. 2. Target engagement of triazoles **10** was evaluated in HEK293 cells using a luminescence protein complementation assay, by measuring FKBP12-FRB dimerization induced with rapamycin. (A) Chemical structures of rapamycin, FK506, and **10b** compounds showing FKBP12 binding groups in red and FRB binding residues in blue. (B) Monitoring of temporal FKBP12/FRB dimerization in HEK293 cells expressing FKBP12 and FRB fused to luciferase fragments. Cells were treated with 100 nM rapamycin (green line), 100 μM FK506 (black line) or 10 mM **10b** compound (red line). RLU, relative light units. (C) Dose-dependent effect of rapamycin on FKBP12-FRB dimerization. In our system, maximal activity was reached with 300 nM rapamycin. (D) Schematics of competition assays. (E) Dose-dependent inhibition of FK506 and **10b** of FKBP12-Rapamycin-FRB interaction induced with 100 nM rapamycin. IC_{50} values were 38.29 μM for FK506 and 3.32 mM for **10b**. Data are expressed as mean \pm SEM of $n = 3-6$ independent experiments performed in triplicate. (F) Target engagement was demonstrated in triazoles **10** (3 mM) where FKBP12/FRB dimerization was induced with 1.2 μM rapamycin. Data are expressed as mean \pm SEM of three measurements. Lower activity values indicate higher inhibition potency.

dehydrogenase release method [32]. All the triazole ligands checked were essentially nontoxic up to millimolar concentration, while S107 was myotoxic at 1 mM concentration (see Supplementary Material, Fig. S2).

3. Conclusions

In this study, we propose a detailed FKBP12/RyR1 interaction mechanism that accounts for the RyR leakage of calcium ion in skeletal muscle fibers under nitro-oxidative stress, that may occur during aging, extreme fatigue, or in several diseases such as Duchenne muscular dystrophy. The model highlights the role of the S-nitrosylated Cys 1781 residue in the peptide segment (Phe-Ser-

Pro-Pro-Cys(NO)-Phe-Val) of the ryanodine receptor RyR1, which compromises the normal peptidyl-prolyl isomerase (PPI) activity of FKBP12 and the calcium conductance of the RyR1 channel. A combination of computational modeling (virtual alanine mutation) and docking studies based on such a model has allowed the identification of polar and hydrophobic hot-spot residues at the FKBP12 protein and the design of a novel family of triazole ligands **10**. Target engagement of several **10** compounds to FKBP12 has been confirmed experimentally using a competitive ligand binding assay with rapamycin. Furthermore, the activity of **10b** compound to enhance the binding of FKBP12 to nitrosylated RyR1 calcium channels has been confirmed experimentally *in vitro* by using *in situ* PLA analysis in healthy human myotubes stressed with the

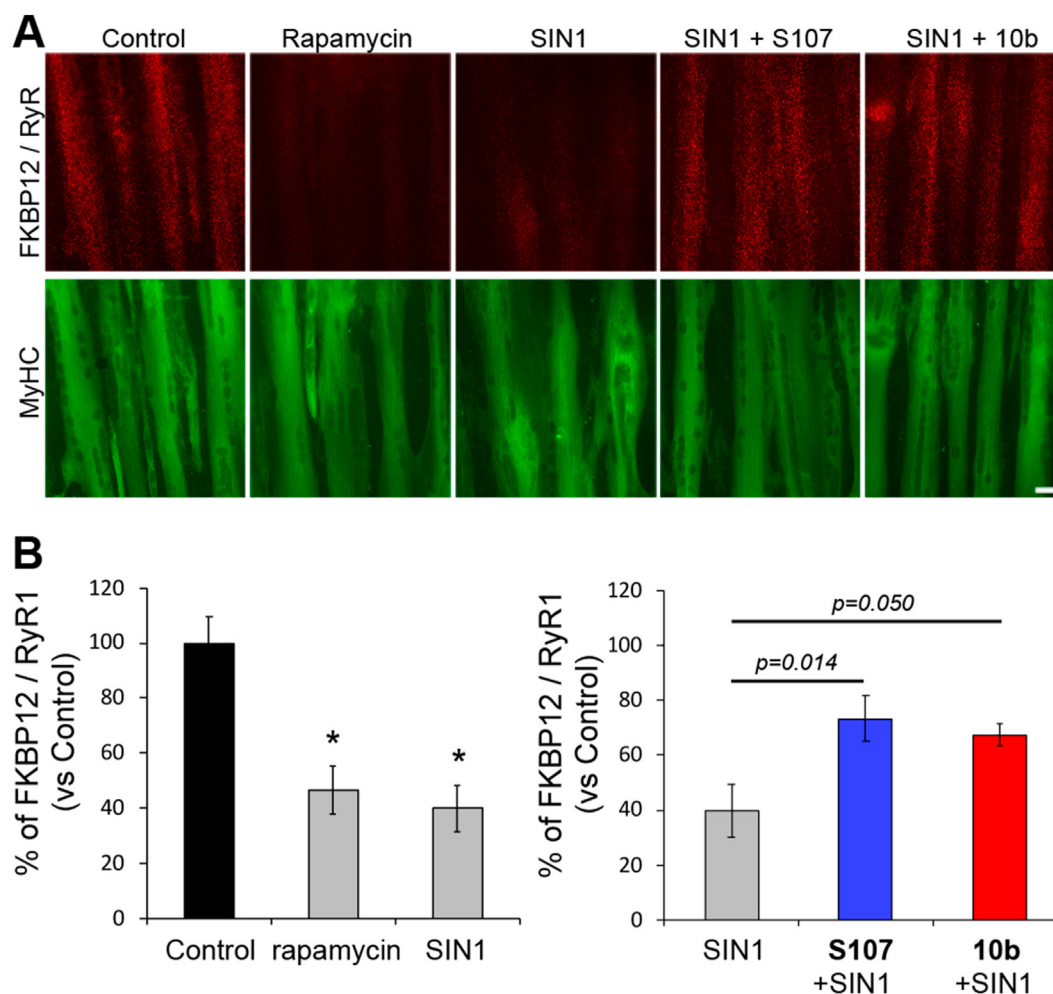


Fig. 3. Triazole **10b** rescues FKBP12/RyR1 co-localization in human myotubes under nitro-oxidative stress. (A) Representative *in situ* proximity ligation assay (PLA) images showing FKBP12/RyR1 co-localization (red) and MyHC double staining (green) in non-stressed myotubes (control), as well as in myotubes stressed with 5 mM SIN1 for 30 min (SIN1). Treatment with S107 and **10b** protective compounds at 150 nM concentration partially rescues SIN1-mediated depletion of FKBP12 from RyR1 complexes. In control myotubes, treatment with 15 μ M rapamycin for 30 min induces a similar FKBP12 depletion from RyR1 complexes as the one observed with SIN1. Scale bar: 25 μ m. (B) Quantification of *in situ* proximity ligation assay (PLA) images showed that both rapamycin and SIN1 (left panel) significantly reduced FKBP12/RyR1 interaction by 53% and 60%, respectively. * $P < 0.0001$ vs. control myotubes. Right panel, reduced FKBP12/RyR1 co-localization in SIN1-stressed myotubes was significantly rescued by pretreatment with S107 or **10b**, with recovery scores (RS) of 56% and 46%, respectively. Data are represented as the percentage of co-localization, where the average of non-treated control myotubes was taken as 100%. Data are expressed as the mean \pm SEM of $n = 11$ – 15 fields from 3 to 4 independent cultures with at least 8 myotubes per field. Statistical significance was determined using one-way ANOVA followed by Dunnett's test.

peroxynitrite-donor SIN1. Finally, we found that some ligands **10** can rescue up to 100% of the normal cytosolic calcium levels in SIN1-stressed human myotube cultures, while showing a lack of substantial toxicity, suggesting that they could minimize the pathogenic effects of nitro-oxidative stress on skeletal muscles. According to these results, the novel triazole ligands described here, and in particular **10b-c**, **10h** or **10iR**, may be useful as therapeutic candidates for the treatment of muscular diseases with compromised calcium homeostasis and/or reduced FKBP12/RyR1 affinity due to nitro-oxidative stress. Further investigation of the *in vivo* activity of compounds **10** in cellular and animal models of Duchenne muscular dystrophy is underway in our laboratories and the results will be reported in due course.

4. Experimental section

4.1. Chemistry

4.1.1. General

All reagents and solvents were obtained from commercial

sources (Merck, Acros Organics, Alfa Aesar, Fluka and Scharlab) and were used without further purification unless stated otherwise. Purification of reaction products was carried out by flash chromatography using silica gel 60 (230–400 mesh). Analytical thin layer chromatography was performed on 0.25 mm silica gel 60-F plates and visualization was accomplished with UV light ($\lambda = 254$ nm) or KMnO_4 as a TLC stain. ^1H NMR spectra were recorded on Bruker Avance spectrometers operated at 500 and 400 MHz. ^{13}C NMR spectra were recorded at 125 and 101 MHz. The chemical shifts are reported as δ values (ppm) relative to residual deuterated solvent as internal standards: for CDCl_3 δ_{H} (7.26 ppm) and δ_{C} (77.16 ppm); for CD_3OD δ_{H} (3.31 ppm) and δ_{C} (49.0 ppm). Analytical HPLC was performed on a Waters 1525 Binary HPLC pump (dual wavelength detector), using a Daicel Chiralpak IC 50 column. The mobile phase was $i\text{PrOH}$ (% 0.1 TFA)/Hex 20:80 with a flow rate of 1 mL/min monitored by UV detection at 210 nm. High-resolution mass spectra were performed by SGIker and were acquired on a time of flight (TOF) mass spectrometer (SYNAPT G2 HDMS from Waters, Milford, MA, USA) equipped with an electrospray source in positive mode (ESI $^+$). Melting points were measured with a Büchi SMP-20

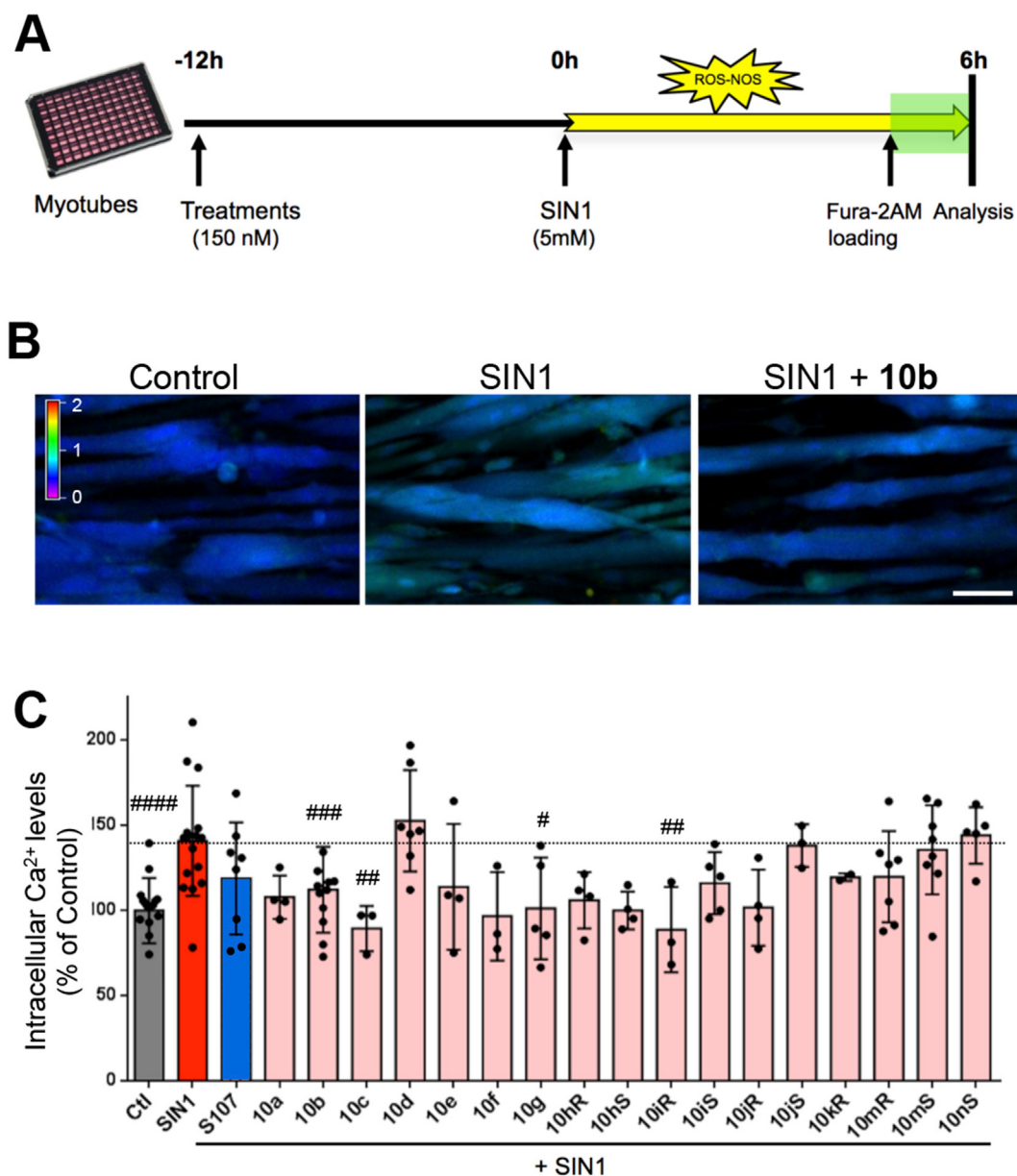


Fig. 4. Triazoles **10a–n** rescue cytosolic calcium levels in SIN1-stressed human myotubes. (A) Schematics of the experimental protocol. (B) Representative pseudocolored images of human myotubes loaded with Fura-2AM fluorochrome showing the F340/380 fluorescence ratio recordings. Scale bar: 50 μm . (C) Quantification of intracellular calcium levels in non-stressed myotubes (Ctl) and myotubes stressed with 5 mM SIN1. All compounds were tested at 150 nM concentration. Data are expressed as mean \pm SD. Each point in the bar chart represents an independent myotube culture, with a minimal analyzed area of 0.325 mm², corresponding to at least 30 myotubes. Statistical significance was determined using one-way ANOVA followed by Dunnett's test, where all groups were compared to the SIN1-stressed group. * $P = 0.05$; ** $P = 0.01$; *** $P = 0.001$; **** $P = 0.0001$.

melting point apparatus and are uncorrected. Infrared spectra were recorded on a Bruker Alpha P. Optical rotations were measured on a Jasco P-200 polarimeter using a sodium lamp (589 nm, D line) at 25 ± 0.2 °C and concentrations are reported in g/mL units.

4.1.2. General procedure for the synthesis of alkynes **1–7**

A suspension of the corresponding thiophenol (10 mmol) and anhydrous K₂CO₃ (21 mmol, 2.90 g) in MeCN (35 mL) was stirred at room temperature for 5 min. Propargyl bromide (15 mmol, 1.67 mL; 80% soln in toluene) was added dropwise and the resulting mixture was heated at 50 °C for 3 h. Quenching with H₂O (10 mL) and evaporation of organic volatiles under reduced pressure provided a solution, which was extracted with CH₂Cl₂ (2 \times 10 mL). The organic extract was washed with brine (10 mL), dried (Na₂SO₄) and

evaporated at reduced pressure to afford a crude product, which was used without further purification in subsequent reactions. Analytically pure samples were obtained by flash column chromatography (silica gel; eluent: hexanes, then MeOH/CH₂Cl₂ 5:95).

4.1.2.1. Phenyl propargyl sulfide (1) [33]. The general procedure was followed starting from thiophenol (10.0 mmol, 1.38 mL). Oil. Yield 0.82 g (56%). ¹H NMR (400 MHz, CDCl₃) δ 7.49 (dt, $J = 8.1, 0.9$ Hz, 2H), 7.40–7.34 (m, 2H), 7.32–7.27 (m, 1H), 2.27 (t, $J = 2.6$ Hz, 1H). ¹³C NMR (101 MHz, CDCl₃) δ 135.2, 130.2, 129.2, 127.2, 80.1, 71.8, 22.8. IR (cm⁻¹): 3289, 1480, 1438, 737, 688, 637.

4.1.2.2. 3-Methoxyphenyl propargyl sulfide (2) [34]. The general procedure was followed starting from 3-methoxybenzenethiol

(10.0 mmol, 1.22 mL). Orange liquid. Yield 1.66 g (93%). ^1H NMR (500 MHz, CDCl_3): δ 7.48 (d, $J = 8.9$ Hz, 2H), 6.87 (d, $J = 8.8$ Hz, 2H), 3.81 (s, 3H), 3.49 (d, $J = 2.6$ Hz, 2H), 2.22 (s, 1H). IR (cm^{-1}): 3286, 1588, 1574, 1245, 1228, 1036, 638.

4.1.2.3. 4-Methoxyphenyl propargyl sulfide (3) [35]. The general procedure was followed starting from 4-methoxybenzenethiol (10.0 mmol, 1.22 mL). Orange solid. Yield 1.95 g (99%). ^1H NMR (500 MHz, CDCl_3): δ 7.30–7.22 (m, 1H), 7.07–6.99 (m, 2H), 6.81 (dd, $J = 7.6, 2.4$ Hz, 1H), 3.83 (s, 3H), 3.65 (s, 2H), 2.27 (t, $J = 2.6$ Hz, 1H). IR (cm^{-1}): 3287, 1590, 1492, 1242, 1026, 823, 636.

4.1.2.4. 3-Chlorophenyl propargyl sulfide (4). The general procedure was followed starting from 3-chlorobenzenethiol (4.68 mmol, 0.54 mL). Yellowish liquid. Yield 0.70 g (82%). ^1H NMR (400 MHz, CDCl_3): δ 7.43 (t, $J = 1.9$ Hz, 1H), 7.31 (dt, $J = 7.5, 1.7$ Hz, 1H), 7.28–7.24 (m, 1H), 7.24–7.20 (m, 1H), 3.62 (d, $J = 2.6$ Hz, 2H), 2.26 (t, $J = 2.6$ Hz, 1H). ^{13}C NMR (101 MHz, CDCl_3): δ 137.1, 134.7, 130.0, 129.3, 127.7, 127.0, 79.3, 72.1, 22.3. IR (cm^{-1}): 3295, 1576, 1460, 1407, 772, 636. MS (ESI-) m/z (%) 180 (M – H). HRMS calculated for ($\text{C}_9\text{H}_6\text{S}$): 180.9879, found 180.9886.

4.1.2.5. 2,3,5,6-Tetrafluorophenyl propargyl sulfide (6). The general procedure was followed starting from 2,3,5,6-tetrafluorobenzenethiol (10 mmol, 1.19 mL). Yellowish liquid. Yield 2.18 g (99%). ^1H NMR (400 MHz, CDCl_3) δ 7.19–7.07 (m, 1H), 3.68 (d, $J = 2.6$ Hz, 2H), 2.22 (t, $J = 2.6$ Hz, 1H). ^{13}C NMR (101 MHz, CDCl_3) δ 148.2, 147.1, 145.8, 144.6, 113.6, 106.8, 78.0, 72.6, 22.5. IR (cm^{-1}): 3306, 1485, 1437, 1240, 1174, 915, 712, 642. IR (cm^{-1}): 3306, 1485, 915, 642.

4.1.2.6. 3-Trifluoromethylphenyl propargyl sulfide (7). The general procedure was followed starting from 3-trifluorobenzenethiol (1 mmol, 1.24 mL). Oil. Yield: 1.10 g (61%). ^1H NMR (400 MHz, CDCl_3) δ 7.73 (s, 1H), 7.67–7.62 (m, 1H), 7.50 (dt, $J = 15.5, 7.7$ Hz, 2H), 3.72–3.64 (m, 2H), 2.29 (dd, $J = 3.2, 2.2$ Hz, 1H). ^{13}C NMR (101 MHz, CDCl_3) δ 136.8, 133.1, 129.6, 126.7, 126.6, 123.9, 123.8, 79.3, 72.4, 22.5. IR (cm^{-1}): 3306, 1320, 1164, 1120, 1070, 792, 694, 648.

4.1.2.7. 4-Methylphenyl 3-butyn-1-yl sulfide (5). Triethylamine (22.5 mmol, 3.1 mL) and methanesulfonyl chloride (22.5 mmol, 1.73 mL) were successively added to a solution of 3-butyn-1-ol (15 mmol, 1.13 mL) in anhydrous CH_2Cl_2 (90 mL) and the mixture was stirred at room temperature overnight. Upon completion (TLC), the organic solution was washed with sat aq NH_4Cl (30 mL), dried over MgSO_4 and evaporated under reduced pressure, to afford crude 3-butyn-1-yl mesylate, which was used in the next step without further purification. 4-Methylbenzenethiol (18.6 mmol, 2.3 g), 3-butyn-1-yl mesylate and anhydrous K_2CO_3 (30 mmol, 4.14 g) were suspended in MeCN (60 mL) and the reaction mixture was heated at 80 °C overnight. After evaporation of the solvents under reduced pressure, the crude product was purified by column chromatography (silica gel; eluent: $\text{CH}_2\text{Cl}_2/\text{MeOH}$, 95:5). Yield: 1.50 g (53%). ^1H NMR (400 MHz, CDCl_3) δ 7.36–7.29 (m, 2H), 7.15 (d, $J = 7.9$ Hz, 2H), 3.05 (t, $J = 7.5$ Hz, 2H), 2.49 (td, $J = 7.5, 2.7$ Hz, 2H), 2.36 (s, 3H), 2.06 (t, $J = 2.6$ Hz, 1H). ^{13}C NMR (101 MHz, CDCl_3) δ 136.8, 131.2, 131.0, 129.8, 82.3, 69.5, 33.5, 21.0, 19.3. IR (cm^{-1}): 3292, 1492, 802, 632, 490.

4.1.3. General procedure for the preparation of achiral triazoles **10a-g** (method A)

A mixture of methyl bromoacetate (1.2 mmol, 113 μL) and sodium azide (1.3 mmol, 84 mg) in MeOH (0.5 mL) and water (0.3 mL) was stirred at 50 °C for 5 h. To this solution was added successively the corresponding alkyne 1–6 (1.0 mmol), dissolved in MeOH/ H_2O

(5 mL: 1 mL), CuOAc (0.05 mmol, 6 mg), NaOAc (3 mmol, 246 mg) and sodium ascorbate (0.5 mmol, 99 mg) and the mixture was stirred at 30 °C overnight. Methanol was evaporated in vacuo, aq 20% ammonia was added (0.25 mL) and the solution was extracted with EtOAc (3×10 mL). The organic extract was washed with a solution sat aq of NH_4Cl (5 mL), dried (Na_2SO_4) and evaporated at reduced pressure. The crude product was purified by column chromatography (silica gel; eluent: EtOAc:Hex mixture) to give the corresponding intermediate triazole methyl ester. To a solution of this compound in THF/ H_2O (4 mL: 4 mL) was added $\text{LiOH} \cdot \text{H}_2\text{O}$ (2.00 mmol, 84 mg) and the mixture was stirred at room temperature for 3 h. The organic solvent was evaporated in vacuo, the resulting aqueous solution was acidified with 1 M HCl and it was extracted with EtOAc (2×10 mL). The combined organic phase was dried (MgSO_4) and evaporated at reduced pressure. The crude products were purified by crystallization in a mixture of EtOAc:hexanes.

4.1.3.1. 1-Carboxymethyl-4-(phenylthiomethyl)-1H-1,2,3-triazole (10a). The general procedure A was followed starting from phenyl propargyl sulfide (**1**) (1.0 mmol, 148 mg). The intermediate methyl ester [^1H NMR (400 MHz, CDCl_3) δ 7.49 (s, 1H), 7.37–7.30 (m, 2H), 7.28–7.24 (m, 2H), 7.23–7.13 (m, 1H), 5.09 (s, 2H), 4.23 (s, 2H), 3.75 (s, 3H). ^{13}C NMR (101 MHz, CDCl_3) δ 166.5, 145.2, 135.2, 129.4, 128.8, 126.3, 123.4, 52.8, 50.5, 28.6] was submitted to saponification to afford the title product. Yield: 80% (198 mg). White solid. Mp: 189–191 °C. ^1H NMR (400 MHz, CD_3OD) δ 7.80 (s, 1H), 7.41–7.35 (m, 2H), 7.34–7.27 (m, 2H), 7.26–7.19 (m, 1H), 5.23 (s, 2H), 4.24 (s, 2H). IR (cm^{-1}): 2413, 1879, 1705, 1232, 690. HRMS calculated for ($\text{C}_{11}\text{H}_{11}\text{N}_3\text{O}_2\text{S}$): 249.0572, found 249.0570.

4.1.3.2. 1-Carboxymethyl-4-(phenylthiomethyl)-1H-1,2,3-triazole (10b). The general procedure A was followed starting from 3-methoxyphenyl propargyl sulfide (**2**) (1.0 mmol, 175 mg). The intermediate methyl ester [^1H NMR (500 MHz, CDCl_3) δ 7.51 (s, 1H), 7.18 (t, $J = 8.0$ Hz, 1H), 6.95–6.86 (m, 2H), 6.77–6.69 (m, 1H), 5.11 (s, 2H), 4.26 (s, 2H), 3.78 (s, 3H), 3.77 (s, 3H). ^{13}C NMR (126 MHz, CDCl_3) δ 166.7, 160.0, 145.7, 136.8, 129.9, 123.6, 121.5, 114.6, 112.5, 55.4, 53.1, 50.8, 28.7] was submitted to saponification to provide the title compound. Yield: 210 mg (74%). White solid. Mp 118–119 °C. ^1H NMR (500 MHz, CD_3OD): δ 7.80 (s, 1H), 7.18 (t, $J = 8.0$ Hz, 1H), 6.96–6.86 (m, 2H), 6.79–6.70 (m, 1H), 5.19 (s, 2H), 4.23 (s, 2H), 3.75 (s, 3H). ^{13}C NMR (126 MHz, CD_3OD): δ 169.7, 161.4, 146.1, 138.0, 130.9, 125.9, 123.1, 116.1, 113.6, 55.7, 51.7, 29.3. IR (cm^{-1}): 2999, 2971, 1707, 1229. MS (ESI+) m/z (%) 280 (M + H). HRMS calculated for ($\text{C}_{12}\text{H}_{14}\text{N}_3\text{O}_4\text{S}$): 280.0756, found 280.0753.

4.1.3.3. 1-Carboxymethyl-4-[4-(methoxy)phenylthiomethyl]-1H-1,2,3-triazole (10c). The general procedure A was followed starting from 4-methoxyphenyl propargyl sulfide (**3**) (1.0 mmol, 175 mg). The intermediate methyl ester [^1H NMR (500 MHz, CDCl_3) δ 7.38 (s, 1H), 7.33–7.28 (m, 2H), 6.85–6.76 (m, 2H), 5.09 (s, 2H), 4.12 (s, 2H), 3.78 (s, 3H), 3.77 (s, 3H). ^{13}C NMR (126 MHz, CDCl_3) δ 166.7, 159.4, 145.8, 134.0, 125.4, 123.5, 114.7, 55.4, 53.1, 50.8, 31.0] was submitted to saponification to afford the title product. Yield: 88% (250 g). White solid. Mp 168–170 °C. ^1H NMR (500 MHz, CD_3OD): δ 7.66 (s, 1H), 7.28 (d, $J = 8.8$ Hz, 2H), 6.84 (d, $J = 8.8$ Hz, 2H), 5.19 (s, 2H), 4.07 (s, 2H), 3.76 (s, 3H). ^{13}C NMR (126 MHz, CD_3OD): δ 169.7, 161.1, 146.3, 135.6, 126.3, 125.9, 115.7, 55.8, 51.6, 31.5. IR (cm^{-1}): 2923, 2848, 1730, 1223, 1188. HRMS calculated for ($\text{C}_{12}\text{H}_{14}\text{N}_3\text{O}_3\text{S}$): 280.0756, found 280.0760.

4.1.3.4. 1-Carboxymethyl-4-[3-(chloro)phenylthiomethyl]-1H-1,2,3-triazole (10d). The general procedure A was followed starting from 3-chlorophenyl propargyl sulfide (**4**) (1.0 mmol, 178 mg). The

intermediate methyl ester [^1H NMR (400 MHz, CDCl_3) δ 7.52 (s, 1H), 7.31 (s, 1H), 7.22–7.13 (m, 3H), 5.12 (s, 2H), 4.26 (s, 2H), 3.79 (s, 3H). ^{13}C NMR (101 MHz, CDCl_3) δ 166.7, 145.2, 137.7, 134.8, 130.2, 129.0, 127.4, 126.7, 123.6, 53.2, 50.9, 28.7] was submitted to saponification to afford the title product. Yield: 67% (0.38 g). White solid. Mp 146–148 °C. ^1H NMR (500 MHz, CDCl_3): δ 7.86 (s, 1H), 7.38 (s, 1H), 7.27 (d, J = 6.8 Hz, 2H), 7.21 (d, J = 1.9 Hz, 1H), 5.22 (s, 2H), 4.28 (s, 2H). ^{13}C NMR (126 MHz, CD_3OD): δ 168.4, 144.2, 137.9, 134.4, 130.0, 128.8, 127.6, 126.3, 124.7, 50.4, 27.7. IR (cm^{-1}): 2928, 2850, 1731, 1224, 1184. MS (ESI+) m/z (%) 284 (M + H). HRMS calculated for ($\text{C}_{11}\text{H}_{10}\text{ClN}_3\text{O}_2\text{S}$): 284.0182, found 284.0190.

4.1.3.5. 1-Carboxymethyl-4-[2-(4-methylphenylthio)ethyl]-1H-1,2,3-triazole (10e). The general procedure A was followed starting from 4-methylphenyl 3-butyn-1-yl sulfide (**5**) (1.0 mmol, 176 mg). The intermediate methyl ester [^1H NMR (400 MHz, CDCl_3) δ 7.53 (s, 1H), 7.35–7.26 (m, 2H), 7.13 (d, J = 7.8 Hz, 1H), 5.16 (s, 2H), 3.82 (s, 3H), 3.23 (t, J = 7.3 Hz, 2H), 3.06 (t, J = 7.4 Hz, 2H), 2.34 (s, 3H). ^{13}C NMR (101 MHz, CDCl_3) δ 167.1, 146.8, 136.8, 132.0, 130.8, 130.0, 123.0, 53.3, 50.9, 34.2, 26.0, 21.2] was submitted to saponification to afford the title product. Yield: 188 mg (68%). White solid. ^1H NMR (400 MHz, CD_3OD): δ 7.84 (s, 1H), 7.31 (d, J = 8.2 Hz, 1H), 7.16 (d, J = 7.9 Hz, 2H), 5.23 (s, 3H), 3.21 (dd, J = 8.0, 6.9 Hz, 2H), 2.99 (t, J = 7.4 Hz, 3H), 2.34 (s, 3H). ^{13}C NMR (101 MHz, CD_3OD): δ 169.8, 147.2, 137.7, 133.3, 131.7, 130.8, 125.3, 51.6, 34.7, 26.6, 21.0. IR (cm^{-1}): 2917, 2500, 2109, 1724, 1215, 803, 486. HRMS calculated for ($\text{C}_{13}\text{H}_{15}\text{N}_3\text{O}_2\text{S}$): 277.0885, found 277.0881.

4.1.3.6. 1-Carboxymethyl-4-[2,3,5,6-(tetrafluoro)phenylthiomethyl]-1H-1,2,3-triazole (10f). The general procedure A was followed starting from 2,3,5,6-tetrafluorophenyl propargyl sulfide (**6**) (1.00 mmol, 220 mg). The intermediate methyl ester [^1H NMR (400 MHz, CDCl_3) δ 7.64 (s, 1H), 7.16–7.01 (m, 1H), 5.16 (s, 2H), 4.29 (s, 2H), 3.83 (s, 3H)] was submitted to saponification to afford the title product. Yield: 292 mg (91%). White solid. M.p.: 205–207 °C. ^1H NMR (500 MHz, CD_3OD): δ 7.88 (s, 1H), 7.43 (tt, J = 10.0, 7.3 Hz, 1H), 5.23 (s, 2H), 4.29 (s, 2H). ^{13}C NMR (126 MHz, CD_3OD): δ 168.2, 147.0 (dt, $^1J_{\text{CF}}$ = 252.0 Hz, $^2J_{\text{CF}}$ = 12.6 Hz), 145.8 (dt, $^1J_{\text{CF}}$ = 243.0 Hz, $^2J_{\text{CF}}$ = 16.4 Hz), 143.7, 124.6, 107.0, 106.8, 106.7, 50.2, 27.9. ^{19}F NMR (471 MHz, CD_3OD): δ -135.73 ($^4J_{\text{FF}}$ = 9.4 Hz) –140.56 ($^4J_{\text{FF}}$ = 9.3 Hz). IR (cm^{-1}): 2435, 1869, 1710, 1486, 1234, 911, 710. HRMS calculated for ($\text{C}_{11}\text{H}_7\text{F}_4\text{N}_3\text{O}_2\text{S}$): 321.0195, found 321.0195.

4.1.3.7. 1-(1-Carboxy-1-methylethyl)-4-[3-(methoxy)phenylthiomethyl]-1H-1,2,3-triazole (10g). A solution of methyl α -bromoisobutyrate (6.6 mmol, 854 μL) and sodium azide (19.8 mmol, 1.3 g) in DMSO (10 mL) was stirred at 50 °C for 2 h. The reaction mixture was quenched with sat aq NaCl (20 mL), extracted with CH_2Cl_2 (2 \times 10 mL) and the organic phase was dried over MgSO_4 , to give methyl α -azidoisobutyrate. To a solution of the crude ester in MeOH/ H_2O (9/3.5 mL) was added 3-methoxyphenyl propargyl sulfide (5.5 mmol, 980 mg), CuOAc (0.28 mmol, 34 mg), NaOAc (16.5 mmol, 1.4 g) and sodium ascorbate (2.75 mmol, 545 mg) and the mixture was stirred at 30 °C overnight. The reaction mixture was worked up and purified according to Method A to provide the corresponding intermediate ester [^1H NMR (400 MHz, CD_3OD): δ 7.77 (s, 1H), 7.09 (t, J = 7.8 Hz, 1H), 6.90–6.73 (m, 2H), 6.67 (d, J = 7.7 Hz, 1H), 4.12 (s, 2H), 3.65 (s, 3H), 1.78 (s, 6H). ^{13}C NMR (101 MHz, CD_3OD): δ 174.2, 161.3, 145.3, 137.9, 130.8, 123.4, 116.5, 113.7, 65.9, 55.7, 29.5, 25.9]. This compound was submitted to saponification with lithium hydroxide monohydrate (2.00 mmol, 84 mg) in THF/ H_2O (4 mL/4 mL) and worked up to provide the title compound. Yield: 72% (138 mg). Brown solid: Mp 119–121 °C. ^1H NMR (400 MHz, CD_3OD): δ 7.77 (s, 1H), 7.09 (t, J = 7.8 Hz, 1H), 6.90–6.73 (m, 2H), 6.67 (d, J = 7.7 Hz, 1H), 4.12 (s, 2H), 3.65 (s, 3H),

1.78 (s, 6H). ^{13}C NMR (101 MHz, CD_3OD): δ 174.2, 161.3, 145.3, 137.9, 130.8, 123.4, 116.5, 113.7, 65.9, 55.7, 29.5, 25.9. IR (cm^{-1}): 2931, 1589, 1573, 1283, 1229, 1178, 1030. MS (ESI+) m/z (%) 308 (M + H). HRMS calculated for ($\text{C}_{14}\text{H}_{18}\text{N}_3\text{O}_3\text{S}$): 308.1069, found 308.1074.

4.1.4. General procedure for the preparation of chiral triazoles **10h-n** (method B)

The corresponding α -amino acid (1.0 mmol) and potassium carbonate (2.0 mmol, 276 mg) were dissolved in a mixture of water (5 mL) and methanol (5 mL). Then, $\text{CuSO}_4 \cdot 5\text{H}_2\text{O}$ (0.01 mmol, 2.5 mg) and 1-(azidosulfonyl)imidazolium hydrogen sulfate **11** (1.1 mmol, 275 mg) were added. The reaction mixture was stirred at room temperature for 5 h to give a solution of the corresponding α -azido acid to which were added successively the corresponding alkyne (**2**), (**4**) or (**7**) (1.2 mmol) dissolved in methanol (1 mL), CuOAc (0.05 mmol, 6 mg), NaOAc (5 mmol, 410 mg) and sodium ascorbate (0.5 mmol, 100 mg). After stirring the mixture overnight at 30 °C, the organic solvent was evaporated in vacuo, pH was adjusted to 10 with a saturated aqueous solution of ammonia and the aqueous phase was washed with CH_2Cl_2 (2 \times 10 mL). The aqueous phase was acidified with 2 M HCl, extracted with EtOAc (2 \times 15 mL) and the extract was dried (MgSO_4) and evaporated at reduced pressure to give the product.

4.1.4.1. (R)-1-(1-Carboxy-2-phenylethyl)-4-[3-(methoxy)phenylthiomethyl]-1H-1,2,3-triazole (10hR). The general procedure B was followed starting from D-phenylalanine (1 mmol, 165 mg) and 3-methoxyphenyl propargyl sulfide (**2**) (1.2 mmol, 213 mg) to give the product. Yield: 76% (280 mg). White solid. Mp 85–86 °C. ^1H NMR (500 MHz, CDCl_3): δ 10.11 (s, 1H), 7.49 (s, 1H), 7.14 (d, J = 7.4 Hz, 4H), 6.89 (d, J = 6.6 Hz, 2H), 6.82 (d, J = 6.7 Hz, 2H), 6.72 (d, J = 7.4 Hz, 1H), 5.53 (dd, J = 9.4, 4.8 Hz, 1H), 4.31–4.08 (m, 2H), 3.70 (s, 3H), 3.52 (dd, J = 14.3, 4.6 Hz, 1H), 3.36 (dd, J = 14.1, 9.8 Hz, 1H). ^{13}C NMR (126 Hz, CD_3OD): δ 171.1, 161.4, 145.9, 138.0, 137.2, 130.9, 129.9, 129.6, 128.1, 124.8, 122.9, 115.9, 113.5, 65.8, 55.7, 39.0, 29.1. IR (cm^{-1}): 2930, 1727, 1246, 1230. MS (ESI+) m/z (%) 384 (M + H). HRMS (ESI+, m/z) calculated for $\text{C}_{19}\text{H}_{20}\text{N}_3\text{O}_3\text{S}$: 370.1225; found: 370.1239. [α] = +16.50 (c 0.98, CH_2Cl_2).

4.1.4.2. (S)-1-(1-Carboxy-2-phenylethyl)-4-[3-(methoxy)phenylthiomethyl]-1H-1,2,3-triazole (10hS). The general procedure B was followed starting from L-phenylalanine (1 mmol, 165 mg) and 3-methoxyphenyl propargyl sulfide (**2**) (1.2 mmol, 213 mg) to give the product. Yield: 73% (270 mg). White solid. Mp 81–83 °C. NMR, IR and HRMS data were identical to example **10hR**. [α] = –23.31 (c 1.12, CH_2Cl_2).

4.1.4.3. (R)-1-(1-Carboxy-3-methylbutyl)-4-[3-(methoxy)phenylthiomethyl]-1H-1,2,3-triazole (10iR). The general procedure B was followed starting from D-leucine (1.1 mmol, 144 mg) and 3-methoxyphenyl propargyl sulfide (**2**) (1.3 mmol, 231 mg) to give the product. Yield: 80% (301 mg). White solid. Mp: 102–104 °C. ^1H NMR (500 MHz, CDCl_3): δ 11.88 (s, 1H), 7.54 (s, 1H), 7.12 (t, J = 7.9 Hz, 1H), 6.95–6.77 (m, 2H), 6.75–6.62 (m, 1H), 5.38 (dd, J = 10.7, 5.0 Hz, 1H), 4.35–4.15 (m, 2H), 3.70 (s, 3H), 2.33–1.75 (m, 2H), 1.17 (dq, J = 13.2, 6.5 Hz, 1H), 0.88 (d, J = 6.5 Hz, 3H), 0.82 (d, J = 6.5 Hz, 3H). ^{13}C NMR (126 Hz, CDCl_3): δ 171.2, 159.8, 144.7, 136.0, 129.8, 122.6, 122.4, 115.6, 112.9, 61.8, 55.3, 41.2, 28.5, 24.7, 22.7, 21.1. IR (cm^{-1}): 2958, 2513, 1726, 1588, 1478, 1229, 1037, 773, 685. MS (ESI+) m/z (%) 336 (M + H). HRMS (ESI+, m/z) calculated for $\text{C}_{16}\text{H}_{22}\text{N}_3\text{O}_3\text{S}$: 336.1382; found: 336.1389. [α] = –12.06 (c 0.95, CH_2Cl_2).

4.1.4.4. (S)-1-(1-Carboxy-3-methylbutyl)-4-[3-(methoxy)phenylthiomethyl]-1H-1,2,3-triazole (10iS). The general procedure B was followed starting from L-leucine (1.1 mmol, 197 mg) and 3-

methoxyphenyl propargyl sulfide (**2**) (1.8 mmol, 320 mg) to give the product. Yield: 75% (360 mg). NMR, IR and HRMS data were identical to example **10iR**. $[\alpha]_D^{24} = +9.31$ (c 1.11, CH₂Cl₂).

4.1.4.5. (*R*)-1-(1-Carboxy-3-methylpropyl)-4-[3-(methoxy)phenylthiomethyl]-1*H*-1,2,3-triazole (**10jR**). The general procedure B was followed starting from *D*-valine (1 mmol, 117 mg) and 3-methoxyphenyl propargyl sulfide (**2**) (1.2 mmol, 213 mg) to give the product. Yield: 69% (220 mg). White solid. Mp 120–123 °C. ¹H NMR (500 MHz, CD₃OD): δ 7.81 (s, 1H), 7.16 (t, *J* = 7.9 Hz, 1H), 7.03–6.82 (m, 2H), 6.82–6.66 (m, 1H), 5.06 (d, *J* = 8.1 Hz, 1H), 4.22 (s, 2H), 3.73 (s, 3H), 2.46 (dt, *J* = 13.5, 6.7 Hz, 1H), 0.95 (d, *J* = 6.7 Hz, 3H), 0.74 (d, *J* = 6.7 Hz, 3H). ¹³C NMR (126 Hz, CD₃OD): δ 170.7, 159.9, 144.6, 136.1, 129.9, 123.0, 122.8, 115.8, 113.0, 69.3, 55.4, 32.2, 28.7, 19.3, 18.3. IR (cm⁻¹): 2966, 2461, 1907, 1591, 1573, 1479, 1281, 1228, 1206, 1037, 783, 721, 687. MS (ESI⁺) *m/z* (%) 336 (M + H). HRMS (ESI⁺, *m/z*) calculated for C₁₅H₂₀N₃O₃S: 332.1227; found: 332.1225. $[\alpha]_D^{24} = -6.68$ (c 1.01, CH₂Cl₂).

4.1.4.6. (*S*)-1-(1-Carboxy-3-methylpropyl)-4-[3-(methoxy)phenylthiomethyl]-1*H*-1,2,3-triazole (**10jS**). The general procedure B was followed starting from *L*-valine (1 mmol, 117 mg) and 3-methoxyphenyl propargyl sulfide (**2**) (1.2 mmol, 259 mg) to give the product. Yield: 65% (210 mg). White solid. Mp 119–121 °C. NMR, IR and HRMS data were identical to example **10jR**. $[\alpha]_D^{24} = +4.52$ (c 1.06, CH₂Cl₂).

4.1.4.7. (*R*)-1-(1-Carboxy-2-phenylethyl)-4-[3-(trifluoromethyl)phenylthiomethyl]-1*H*-1,2,3-triazole (**10kR**). The general procedure B was followed starting from *D*-phenylalanine (1 mmol, 165 mg) and 3-trifluoromethylphenyl propargyl sulfide (**7**) (1.2 mmol, 259 mg) to give the product. Yield: 63% (258 mg) 81% (329 mg). Oil. ¹H NMR (500 MHz, CD₃OD): δ 7.85 (s, 1H), 7.61 (s, 1H), 7.56–7.42 (m, 3H), 7.13 (dd, *J* = 5.0, 2.0 Hz, 2H), 7.04–6.95 (m, 2H), 5.62 (dd, *J* = 10.8, 4.7 Hz, 1H), 4.27 (s, 2H), 3.61 (dd, *J* = 14.4, 4.7 Hz, 1H), 3.45 (dd, *J* = 14.3, 10.8 Hz, 1H). ¹³C NMR (126 MHz, CD₃OD) δ 169.6, 143.8, 137.3, 135.7, 132.4, 132.3, 130.9 (q, ²*J*_{CF} = 31.0 Hz), 129.4, 128.5, 128.2, 126.7, 125.4, 125.3, 123.9 (q, ¹*J*_{CF} = 271.0 Hz), 123.6, 122.7, 122.6, 122.5, 64.3, 37.5, 27.3. ¹⁹F NMR (471 MHz, CD₃OD): δ -64.26. IR (cm⁻¹): 1716, 1319, 1122, 692. HRMS (ESI⁺, *m/z*) calculated for C₁₉H₁₇N₃O₂SF₃: 408.0994; found: 408.1005. $[\alpha]_D^{24} = +16.8^\circ$ (c. 0.98 g/100 mL, CH₂Cl₂).

4.1.4.8. (*R*)-1-[1-Carboxy-2-(4-hydroxyphenyl)ethyl]-4-[3-(trifluoromethyl)phenylthiomethyl]-1*H*-1,2,3-triazole (**1mR**). The General Procedure B was followed starting from *D*-tyrosine (1 mmol, 181 mg) and 3-trifluoromethylphenyl propargyl sulfide (**7**) (1.2 mmol, 259 mg) to give the product. Yield: 73% (308 mg). Oil. ¹H NMR (400 MHz, CD₃OD): δ 7.84 (s, 1H), 7.62 (s, 1H), 7.53–7.39 (m, 3H), 6.84–6.77 (m, 2H), 6.58 (d, *J* = 8.5 Hz, 2H), 5.54 (dd, *J* = 10.5, 4.7 Hz, 1H), 4.25 (s, 2H), 3.49 (dd, *J* = 14.4, 4.7 Hz, 1H), 3.39–3.29 (m, 1H). ¹³C NMR (126 MHz, CD₃OD) δ 167.7, 156.5, 135.7, 133.4, 131.0 (q, ²*J*_{CF} = 32.0 Hz), 129.8, 129.6, 129.5, 126.4, 125.3, 125.2, 123.8 (q, ¹*J*_{CF} = 274.7 Hz), 123.5, 115.3, 65.9, 62.5, 36.4. ¹⁹F NMR (471 MHz, CD₃OD): δ -64.01. IR (cm⁻¹): 2924 br, 1732, 1516, 1321, 1164, 1120, 1067, 792, 695. HRMS (ESI⁺) *m/z* calculated for C₁₉H₁₇N₃O₃SF₃: 424.0943; found: 424.0949. $[\alpha]_D^{24} = +28.7^\circ$ (c. 1.14 g/100 mL, MeOH).

4.1.4.9. (*S*)-1-[1-Carboxy-2-(4-hydroxyphenyl)ethyl]-4-[3-(trifluoromethyl)phenylthiomethyl]-1*H*-1,2,3-triazole (**1mS**). The General Procedure B was followed starting from *L*-tyrosine (1 mmol, 181 mg) and 3-trifluoromethylphenyl propargyl sulfide (**7**) (1.2 mmol, 259 mg) to give the product. Yield: 86% (318 mg). Oil. NMR, IR and HRMS data were identical to example **10mR**

$[\alpha]_D^{24} = -32.10^\circ$ (c. 1.21 g/100 mL, MeOH).

4.1.4.10. (*S*)-1-[5-*tert*-Butoxycarbonylamino-1-carboxypentyl]-4-[3-(chloro)phenylthiomethyl]-1*H*-1,2,3-triazole (**10nS**). The general procedure B was followed starting from *N*-Boc-*L*-lysine (1 mmol, 246 mg) and 3-chlorophenyl propargyl sulfide (**4**) (1.2 mmol, 219 mg) to give the product. Yield: 63% (286 mg). Oil. ¹H NMR (400 MHz, CD₃CN) δ 7.76 (s, 1H), 7.43 (q, *J* = 1.3 Hz, 1H), 7.32–7.28 (m, 2H), 7.25 (qt, *J* = 4.8, 2.2 Hz, 1H), 5.29 (dd, *J* = 10.4, 5.0 Hz, 1H), 4.30 (s, 2H), 2.97 (qd, *J* = 6.8, 2.9 Hz, 2H), 2.30–2.07 (m, 2H), 1.41 (s, 11H), 1.03 (tt, *J* = 8.7, 4.4 Hz, 2H). $[\alpha]_D^{24} = -9.8^\circ$ (c. 0.95 g/100 mL, MeOH). IR (cm⁻¹): 2976, 1684, 1180, 1152, 778, 607. HRMS calculated for (C₂₀H₂₇ClN₄O₄S): 454.1442, found 454.1458.

4.2. Biological evaluation

4.2.1. Cell cultures

LHCN-M2 and 8220 immortalized human myoblasts were kindly provided by Dr. Vincent Mouly (Myology Institute, Paris). These cells were generated by the Platform for Immortalization of Human Cells (Myology Institute, Paris). Human myoblasts were grown and differentiated as previously reported [36]. Experiments were performed 7–9 days after first adding differentiation medium, with highly mature myotubes.

4.2.2. Competitive ligand binding assay

HEK293 cells were seeded onto white 96-well plates (Corning) coated with poly-*D*-lysine at 4 × 10⁵ cells per well. Cells were grown in DMEM (Thermofisher) with 10% FBS for 6 h and transfected with 12.5 ng/μL of each FRB-IgBiT and FKBP-smBiT vectors (NanoBiT Control Pair, Promega) using ViaFect. Kinetic measurements were performed 20–24 h after transfection in CO₂ Independent Medium (Gibco, Thermofisher) with Nano-Glo® Live Cell Reagent (Promega), as described by the manufacturer. Luminescence was measured at 37 °C using the Glomax Discover Microplate Reader (Promega). Rapamycin, FK506 and triazole compounds were sequentially added and each effect was recorded for 15 min. To establish the specific activity in competitive binding assays, measured values of basal activity (BA) at 10 min, maximal activity (MA) at 25 min, and compound activity (CA) at 40 min were determined. Specific activity (SA) was calculated using the formula: SA = (MA-BA)/(CA-BA)*100. SA was normalized to the nondrug (vehicle) measurements. IC₅₀ and EC₅₀ were calculated in GraphPad Prism 8.0.1 by fitting the data to a four-parameter logistic curve.

4.2.3. In situ proximity ligation assay (PLA)

In situ PLA assay was performed as previously described [37]. Briefly, paraformaldehyde-fixed myotubes were blocked and incubated overnight with the following primary antibodies: anti-RyR1 mouse mAb (1:200, Thermo Scientific), and anti-Calst1 rabbit pAb (1:100, Novus Biologicals). PLA assay was performed using the Duolink *in situ* Orange kit (Sigma). Samples were incubated with oligonucleotide strand conjugated secondary antibodies (MINUS and PLUS PLA probes, Sigma). For counterstaining, samples were incubated with FITC-conjugated Myosin Heavy Chain-CFS mAb (1:50, R&D) for 30 min, and mounted with ProLong Gold antifade reagent with DAPI (Life Technologies). Image quantification was performed with ImageJ (NIH) and the “Batch spot analysis” macro from the Henry Wellcome Laboratory (<https://www.uea.ac.uk/about/faculties-and-schools/faculty-of-science/facilities/bio-imaging-platform/macros>). For each image, the total number of spots was normalized to the MyHC area. At least 4 images per condition were analyzed with an average of 8–9 myotubes per image.

4.2.4. Calcium imaging

Calcium imaging was performed as previously described [36,37]. Briefly, control human 8220 myotubes differentiated for 9 days were pre-treated with S107 and triazole compounds **10a-n** (150 nM) for 12 h. Then, nitro-oxidative stress was induced with 5 mM SIN1 (3-morpholino-sydonimine chloride) for 6 h. Intracellular calcium levels were analyzed by loading 8220 myotubes with the ratiometric fluorochrome Fura-2AM (4 μ M) and pluronic acid (0.02%) for 30 min at 37 °C. Myotubes were visualized with a high-resolution camera and calcium levels were estimated from the excitation ratio 340 nm/380 nm. Each group comprised 6 replicates and at least 4 images were analyzed from each sample. $N \geq 30$ myotubes per group. Data were expressed as mean \pm SEM. To measure the activity of compounds, the recovery score was determined on the formula [38]: Recovery Score (%) = (Treated-non treated)/(Control-non treated) \times 100.

4.2.5. Statistical analyses

Data was evaluated for normal distribution using Shapiro-Wilk and D'Agostino & Pearson tests (GraphPad Prism 8.0.1). Outliers were identified with Grubbs' test and they were excluded from subsequent statistical analyses. Statistical significance was determined using the Student's *t*-test or One-Way ANOVA followed by Dunnett's or Tukey's multiple comparisons test. *P*-values ≤ 0.05 were considered statistically significant.

Declaration of competing interest

The authors declare that they have no known competing financial interests or personal relationships that could have appeared to influence the work reported in this paper.

Acknowledgments

This research was funded by the Basque Government (J.M.A., GIC-2015_IT-1033-16; J.M.A., ETORTEK-KK-2018/00108; A.V.-I., 2016111091); Instituto de Salud Carlos III, co-funded by European Regional Development Fund/European Social Fund, "Investing in your future" (A.V.-I., PI17/00676; A.L.d.M., PI17/01841), Diputación Foral de Gipuzkoa (A.V.-I., 2019-00362-01-B); the University of the Basque Country (A.V.-I., PPGA19/58, PPGA20/23), and Duchenne Parent Project, España (A.V.-I.). A.S.-A., A.I., G.A. hold fellowships from the Basque Government, H.L.-F. holds a PhD fellowship from the UPV/EHU and A.V.-I. holds a Ramón y Cajal contract funded by the Spanish Ministry of Economy and Competitiveness. The authors thank Dr. Mouly and the Platform for Immortalization of Human Cells (Myology Institute) for the human LHCN-M2 and 8220 cell lines. The use of SGlker NMR facilities is acknowledged to the University of the Basque Country UPV/EHU.

Appendix A. Supplementary data

Supplementary data to this article can be found online at <https://doi.org/10.1016/j.ejmech.2021.113160>.

References

- [1] K.P. Lu, G. Finn, T.H. Lee, L.K. Nicholson, Prolyl *cis-trans* isomerization as a molecular timer, *Nat. Chem. Biol.* 3 (2007) 619–629.
- [2] I.Y. Kuo, B.E. Ehrlich, Muscling in on the ryanodine receptor, *Nat. Struct. Mol. Biol.* 22 (2015) 106–107.
- [3] A.M. Bellinger, S. Reiken, M. Dura, P.W. Murphy, S.-X. Deng, D.W. Landry, D. Nieman, S.E. Lehnart, M. Samaru, A. LaCampagne, A.R. Marks, Remodeling of ryanodine receptor complex causes "leaky" channels: a molecular mechanism for decrease exercise capacity, *Proc. Natl. Acad. Sci. U.S.A.* 105 (2008) 2198–2202.
- [4] A.M. Bellinger, M. Mongillo, A.R. Marks, Stressed out: the skeletal muscle

- ryanodine as a target of stress, *J. Clin. Invest.* 118 (2008) 445–453.
- [5] T. Murayama, N. Kurebayashi, M. Ishigami-Yuasa, S. Mori, Y. Suzuki, R. Akima, H. Ogawa, J. Suzuki, K. Kanemura, H. Oyama, Y. Kiuchi, M. Iino, H. Kagechika, T. Sakurai, Efficient high-throughput screening by endoplasmic reticulum Ca²⁺ measurement to identify inhibitors of ryanodine receptor Ca²⁺-release channels, *Mol. Pharmacol.* 94 (2018) 722–730.
- [6] J.S. Stalmer, Q.-A. Sun, D.T. Hess, A SNO storm in skeletal muscle, *Cell* 133 (2008) 33–35.
- [7] E. Murphy, M. Kohr, J. Sun, T. Nguyen, C. Steenbergen, S-nitrosylation: a radical way to protect the heart, *J. Mol. Cell. Cardiol.* 52 (2012) 568–577.
- [8] R. Zalk, O.B. Clarke, A. des Georges, R.A. Grassucci, S. Reiken, F. Mancina, W.A. Hendrickson, J. Frank, A.R. Marks, Structure of a mammalian ryanodine receptor, *Nature* 517 (2015) 44–49.
- [9] Z. Yan, X.-Ch Bai, Ch Yan, J. Wu, Z. Li, T. Xie, W. Peng, Ch-Ch Yin, X. Li, S.H.W. Scheres, Y. Shi, N. Yan, Structure of the rabbit ryanodine receptor RyR1 at near-atomic resolution, *Nature* 517 (2015) 50–55.
- [10] X.-Ch Bai, Z. Yan, J. Wu, Z. Li, N. Yan, The central domain of RyR1 is the transducer for long-range allosteric gating of channel opening, *Cell Res.* 26 (2016) 995–1006.
- [11] W. Zheng, Toward decrypting the allosteric mechanism of the ryanodine receptor based on coarse grained structural and dynamic modeling, *Proteins* 83 (2015) 2307–2318.
- [12] M. Albers, C.T. Walsh, L. Schreiber, Substrate specificity for the human rotamase FKBP: a view of FK506 and rapamycin as leucine-(twisted amide)-proline mimics, *J. Org. Chem.* 55 (1990) 4984–4986.
- [13] S. Fischer, S. Michnick, M. Karplus, A mechanism for rotamerase catalysis by the FK506 binding protein (FKBP), *Biochemistry* 32 (1993) 13830–13837.
- [14] M. Orozco, J. Tirado-Rives, W.L. Jorgensen, Mechanism for the rotamerase activity of FK506 binding protein from molecular dynamics simulations, *Biochemistry* 32 (1993) 12864–12874.
- [15] (a) X.J. Wang, F.A. Etzkorn, Peptidyl-prolyl isomerase inhibitors, *Biopolymers* 84 (2006) 125–146; (b) B.M. Duniak, J.E. Gestwicki, Peptidyl-proline isomerases (PPIases): targets for natural products and natural product-inspired compounds, *J. Med. Chem.* 59 (2016) 9622–9644.
- [16] A.B. Brillantes, K. Ondrias, A. Scott, E. Kobrin, E. Ondriasová, M.C. Moschella, T. Jayaraman, M. Landers, B.E. Ehrlich, A.R. Marks, Stabilization of calcium release channel (ryanodine receptor) function by FK506-binding protein, *Cell* 77 (1994) 513–523.
- [17] (a) N. Kaneko, R. Matsuda, Y. Hata, K. Shimamoto, Pharmacological characteristics and clinical applications of K201, *Curr. Clin. Pharmacol.* 4 (2009) 126–131; (b) X.H.T. Wehrens, S.E. Lehnart, S. Reiken, R. Van der Nagel, R. Morales, J. Sun, Z. Cheng, S.-X. Deng, L.J. Windt, D.W. Landry, A.R. Marks, Enhancing calstabin binding to ryanodine receptors improves cardiac and skeletal muscle function in heart failure, *Proc. Natl. Acad. Sci. U.S.A.* 102 (2005) 9607–9612.
- [18] Y. Mei, L. Xu, H.F. Kramer, G.H. Tomberlin, C. Townsend, G. Meissner, Stabilization of the skeletal muscle ryanodine receptor ion channel-FKBP12 complex by the 1,4-benzothiazepine derivative S107, *PLoS One* 8 (2013), e54208.
- [19] R.F. Capogrosso, P. Mantuano, K. Uaesoontrachoon, A. Cozzoli, A. Giustino, T. Dow, S. Srinivassane, M. Filipovic, C. Bell, J. Vandermeulen, A.M. Massari, M. De Bellis, E. Conte, S. Pierno, G.M. Camerino, A. Liantonio, K. Nagaraju, A. De Luca, Ryanodine channel complex stabilizer compound S48168/ARM210 as a disease modifier in dystrophin-deficient mdx mice: proof-of-concept study and independent validation of efficacy, *Faseb. J.* 32 (2018) 1025–1043.
- [20] A.M. Bellinger, S. Reiken, C. Carlson, M. Mongillo, X. Liu, L. Rothman, S. Matecki, A. LaCampagne, A.R. Marks, Hypernitrosylated ryanodine receptor calcium release channels are leaky in dystrophic muscle, *Trends Mol. Med.* 15 (2009) 2198–2202.
- [21] Y. Yan, D. Zhang, P. Zhou, B. Li, S.-Y. Huang, HDock: a web server for protein-protein and protein DNA/RNA docking based on a hybrid strategy, *Nucleic Acids Res.* 45 (2017) W365–W373.
- [22] A. Massarotti, S. Aprile, V. Mercalli, E. Del Grosso, G. Grosa, G. Sorba, G.C. Tron, Are 1,4- and 1,5-disubstituted 1,2,3-triazoles good pharmacophoric groups? *ChemMedChem* 9 (2014) 2497–2508.
- [23] (a) P.A. Ravindranath, S. Forli, D.S. Goodsell, A.J. Olson, M.F. Sanner, AutoDockFR: advances in protein-ligand docking with explicitly specified binding site flexibility, *PLoS Comput. Biol.* 11 (2015), e1004586; (b) Y. Zhao, D. Stoffer, M. Sanner, Hierarchical and multi-resolution representation of protein flexibility, *Bioinformatics* 22 (2006) 2768–2774.
- [24] H. Johansson, D.S. Pedersen, Azide- and alkyne-derivatised α -amino acids, *Eur. J. Org. Chem.* (2012) 4267–4281.
- [25] (a) E.D. Goddard-Borger, R.V. Stick, An efficient, inexpensive and shelf-stable diazotransfer reagent: imidazole-1-sulfonyl azide hydrochloride, *Org. Lett.* 9 (2007) 3797–3800; (b) N. Fischer, E.D. Goddard-Borger, R. Greiner, T.M. Klapöke, B.W. Skelton, J. Stierstofer, Sensitivities of some imidazole-1-sulfonyl azide salts, *J. Org. Chem.* 77 (2012) 1760–1764.
- [26] A.S. Dixon, M.K. Schwinn, M.P. Hall, K. Zimmerman, P. Otto, T.H. Lubben, B.L. Butler, B.F. Binkowski, T. Machleidt, T.A. Kirkland, M.G. Wood, C.T. Eggers, L.P. Encell, K.V. Wood, NanoLuc complementation reporter optimized for accurate measurement of protein interactions in cells, *ACS Chem. Biol.* 11 (2016) 400–408.
- [27] L.A. Banaszynski, C.W. Liu, T.J. Wandless, Characterization of the FKBP, rapamycin, FRB ternary complex, *J. Am. Chem. Soc.* 127 (2005) 4715–4721.

- [28] R.J. Singh, N. Hogg, J. Joseph, E. Konorev, B. Kalyanaraman, The peroxydinitrate generator, SIN-1, becomes a nitric oxide donor in the presence of electron acceptors, *Arch. Biochem. Biophys.* 361 (1999) 331–339.
- [29] S. Kakizawa, Nitric oxide-induced calcium release: activation of type 1 ryanodine receptor, a calcium release channel, through non-enzymatic post-translational modification by nitric oxide, *Front. Exp. Endocrinol.* 4 (2013) 142.
- [30] (a) O. Söderberg, M. Gullberg, M. Jarvius, K. Ridderstrale, K.-J. Leuchowius, J. Jarvius, K. Wester, P. Hydbring, F. Bahram, L.-G. Larsson, U. Landegren, Direct observation of individual endogenous protein complexes *in situ* by proximity ligation, *Nat. Methods* 3 (2006) 995–1000;
(b) C. Greenwood, D. Ruff, S. Kirvell, G. Johnson, H.S. Dhillon, S.A. Bustin, Proximity assays for sensitive quantification of proteins, *Biomol. Detect. Quantif.* 4 (2015) 10–16.
- [31] F. Van Petegem, Ryanodine receptors: allosteric ion channel giants, *J. Mol. Biol.* 427 (2015) 31–53.
- [32] A.L. Niles, R.A. Moravec, T.L. Riss, In vitro viability and cytotoxicity testing and same-well multi-parametric combinations for high throughput screening, *Curr. Chem. Genom.* 3 (2009) 33–41.
- [33] (a) T. Martzel, J.F. Lohier, A.C. Gaumont, J.F. Briere, S. Perrio, Sulfinate-organocatalyzed (3+2) annulation reaction of progargyl or allenyl sulfones with activated imines, *Eur. J. Org. Chem.* 36 (2018) 5069–5073;
(b) S.E. Denmark, M.A. Harmata, K.S. White, Studies on the addition of allyl oxides to sulfonyllallenes. Preparation of highly substituted allyl vinyl ethers for carbanionic Claisen rearrangements, *J. Org. Chem.* 52 (1987) 4031–4042.
- [34] J.T. Lundquist IV, J. Pelletier, Improved solid-phase peptide synthesis method utilizing α -azide-protected amino acids, *Org. Lett.* 3 (2001) 781–783.
- [35] D. Yadagiri, P. Anbarasan, Tandem 1,2-sulfur migration and (aza)-Diels-Alder reaction of β -thio- α -diazimines: rhodium catalyzed synthesis of (fused)-polyhydropyridines and cyclohexenes, *Chem. Sci.* 6 (2015) 5847–5852.
- [36] I. Toral-Ojeda, G. Aldanondo, J. Lasa-Elgarresta, H. Lasa-Fernández, R. Fernández-Torrón, A. López de Munain, A. Vallejo-Illarramendi, Calpain 3 deficiency affects SERCA expression and function in the skeletal muscle, *Expet Rev. Mol. Med.* 18 (2016) e7, <https://doi.org/10.1017/erm.2016.9>.
- [37] I. Toral-Ojeda, G. Aldanondo, J. Lasa-Elgarresta, H. Lasa-Fernández, C. Vesga-Castro, V. Mouly, A. López de Munain, A. Vallejo-Illarramendi, A novel functional in vitro model that recapitulates human muscle disorders, in: K. Sakuma (Ed.), *Muscle Cell and Tissue - Current Status of Research Field*, 2018, <https://doi.org/10.5772/intechopen.75903>.
- [38] J.-M. Gillis, Multivariate evaluation of the functional recovery obtained by the overexpression of utrophin in skeletal muscles of the *mdx* mouse, *Neuromuscul. Disord.* 12 (2002) S09–S94.